PHYSICAL REVIEW D **78,** 063520 (2008)

Predicting the cosmological constant with the scale-factor cutoff measure

Andrea De Simone,[1] Alan H. Guth,[1] Michael P. Salem,[2] and Alexander Vilenkin[2]

[1]*Center for Theoretical Physics, Laboratory for Nuclear Science, and Department of Physics, Massachusetts Institute of Technology, Cambridge, Massachusetts 02139, USA*

[2]*Institute of Cosmology, Department of Physics and Astronomy, Tufts University, Medford, Massachusetts 02155, USA*

(Received 30 May 2008; published 12 September 2008)

It is well known that anthropic selection from a landscape with a flat prior distribution of cosmological constant Λ gives a reasonable fit to observation. However, a realistic model of the multiverse has a physical volume that diverges with time, and the predicted distribution of Λ depends on how the spacetime volume is regulated. A very promising method of regulation uses a scale-factor cutoff, which avoids a number of serious problems that arise in other approaches. In particular, the scale-factor cutoff avoids the ''youngness problem'' (high probability of living in a much younger universe) and the ''Q and G catastrophes'' (high probability for the primordial density contrast Q and gravitational constant G to have extremely large or small values). We apply the scale-factor cutoff measure to the probability distribution of Λ, considering both positive and negative values. The results are in good agreement with observation. In particular, the scale-factor cutoff strongly suppresses the probability for values of Λ that are more than about 10 times the observed value. We also discuss qualitatively the prediction for the density parameter Ω, indicating that with this measure there is a possibility of detectable negative curvature.

DOI: 10.1103/PhysRevD.78.063520 PACS numbers: 98.80.Cq

I. INTRODUCTION

The present understanding of inflationary cosmology suggests that our Universe is one among an infinite number of ''pockets'' in an eternally inflating multiverse. Each of these pockets contains an infinite, nearly homogeneous and isotropic universe and, when the fundamental theory admits a landscape of metastable vacua, each may be characterized by different physical parameters, or even different particles and interactions, than those observed within our pocket. Predicting what physics we should expect to observe within our region of such a multiverse is a major challenge for theoretical physics. (For recent reviews of this issue, see e.g. [1–5].)

The attempt to build a calculus for such predictions is complicated in part by the need to regulate the diverging spacetime volume of the multiverse. A number of different approaches to this measure problem have been explored: a cutoff at a fixed global time [6–8],[1] the so-called ''gauge-invariant'' measures [11,12], where different cutoff times are used in different pockets in order to make the measure approximately time-parametrization invariant, the pocket-based measure [13–16], which avoids reference to global time by focusing on pocket abundances and regulates the diverging volume within each pocket with a spherical volume cutoff, and finally the causal-patch measures [17,18], which restrict consideration to the spacetime volume accessible to a single observer.[2] Different measures make different observational predictions. To help decide which, if any, is on the right track, one can take an empirical approach, working out the predictions of candidate measures and comparing them with observation. Although currently available predictions are not precise enough to determine the measure, many proposals can be rejected due to clear conflicts with observation, and in other cases the quantitative predictions can at least be suggestive. In this spirit, we investigate one of the simplest global-time measure proposals: the scale-factor cutoff measure.

To begin, we discuss the predictions of the scale-factor cutoff measure for issues that have proven problematic for many other measures. For example, another member of the global-time measure family—the proper-time cutoff measure—predicts a population of observers that is extremely youth-dominated [2,21,22]. Observers who take a little less time to evolve are hugely more numerous than their slower-evolving counterparts, suggesting that we should most likely have evolved at a very early cosmic time, when the conditions for life were rather hostile. This counterfactual prediction is known as ''the youngness paradox.'' Furthermore, the ''gauge-invariant'' and pocket-based

[1]Much of the early work sought to calculate the relative volumes occupied by different pockets on hypersurfaces of constant time [9,10]. In Ref. [6] the probabilities were expressed in terms of the fluxes appearing in the Fokker-Planck equation for eternal inflation. In most (but not all) cases, this method is equivalent to imposing a cutoff at a constant time. The prescription of a global-time cutoff was first explicitly formulated in [7].

[2]We also note the recent measure proposals in Refs. [19,20]. Observational predictions of these measures have not yet been worked out, so we shall not discuss them any further.

measures suffer from a "Q catastrophe," exponentially preferring either very large or very small values of the primordial density contrast Q [23,24]. In fact, this problem is not restricted to Q—there are similar expectations for the gravitational constant G [25]. We show that the youngness bias is very mild in the scale-factor cutoff, and that there is no Q (or G) catastrophe. We also describe qualitative expectations for the distributions of Q and of the density parameter Ω.

The above considerations establish the scale-factor cutoff as a promising candidate for the spacetime measure, motivating the study of its more detailed predictions. The main focus of this paper is on the prediction of the cosmological constant Λ [7,26–30], which is arguably a major success of the multiverse picture. Most calculations of the distribution of Λ in the literature [29–34] do not explicitly specify the measure, but in fact correspond to using the pocket-based measure. The distribution of positive Λ in a causal-patch measure has also been considered [35,36]. The authors of Ref. [35] emphasize that the causal-patch measure gives a strong suppression for values of Λ more than about 10 times the observed value, while anthropic constraints alone might easily allow values 1000 times larger than observed, depending on assumptions. Here, we calculate the distribution for Λ in the scale-factor cutoff measure, considering both positive and negative values of Λ, and compare our results with those of other approaches. We find that our distribution is in a good agreement with the observed value of Λ, and that the scale-factor cutoff gives a suppression for large positive values of Λ that is very similar to that of the causal-patch measure.

This paper is organized as follows. In Sec. II we describe the scale-factor cutoff, commenting on its more salient features, including its very mild youngness bias and aspects of the distributions of Q and Ω. In Sec. III we compute the probability distribution of Λ, calculating it first for the pocket-based measure, reproducing previous results, and then calculating it for the scale-factor cutoff. In both cases we study positive and negative values of Λ. Our main results are summarized in Sec. IV. Finally, we include two appendices. In Appendix A we consider the possibility that the landscape splits into several disconnected sectors, and show that even in this situation the scale-factor cutoff measure is essentially independent of the initial state of the Universe. Appendix B contains an analysis of the evolution of the collapse density threshold, along with a description of the linear growth function of density perturbations.

II. THE SCALE-FACTOR CUTOFF

A. Global-time cutoffs

To introduce a global-time cutoff, we start with a patch of a spacelike hypersurface Σ somewhere in the inflating part of spacetime, and follow its evolution along the congruence of geodesics orthogonal to Σ. The spacetime region covered by this congruence will typically have infinite spacetime volume, and will include an infinite number of pockets. In the global-time cutoff approach we introduce a time coordinate t, and restrict our attention to the finite spacetime region $\Gamma(\Sigma, t_c)$ swept out by the geodesics prior to $t = t_c$, where t_c is a cutoff which is taken to infinity at the end of the calculation. The relative probability of any two types of events A and B is then defined to be

$$\frac{p(A)}{p(B)} \equiv \lim_{t_c\to\infty} \frac{n(A, \Gamma(\Sigma, t_c))}{n(B, \Gamma(\Sigma, t_c))}, \tag{1}$$

where $n(A, \Gamma)$ and $n(B, \Gamma)$ are the number of events of types A and B, respectively, in the spacetime region Γ. In particular, the probability P_j of measuring parameter values corresponding to a pocket of type j is proportional to the number of independent measurements made in that type of pocket, within the spacetime region $\Gamma(\Sigma, t_c)$, in the limit $t_c \to \infty$.

The time coordinate t is "global" in the sense that constant-time surfaces cross many different pockets. Note, however, that it does not have to be global for the entire spacetime, so the initial surface Σ does not have to be a Cauchy surface for the multiverse. It need not be monotonic, either, where for nonmonotonic t we limit $\Gamma(\Sigma, t_c)$ to points along the geodesics prior to the first occurrence of $t = t_c$.

As we will discuss in more detail in Appendix A, probability distributions obtained from this kind of measure are independent of the choice of the hypersurface Σ.[3] They do depend, however, on how one defines the time parameter t. To understand this sensitivity to the choice of cutoff, note that the eternally inflating universe is rapidly expanding, such that at any time most of the volume is in pockets that have just formed. These pockets are therefore very near the cutoff surface at $t = t_c$, which explains why distributions depend on exactly how that surface is drawn.

A natural choice of the time coordinate t is the proper time τ along the geodesic congruence. But as we have already mentioned, and will discuss in more detail in the following subsection, this choice is plagued with the youngness paradox, and therefore does not yield a satisfactory measure. Another natural option is to use the expansion factor a along the geodesics as a measure of time. The scale-factor time is then defined as

$$t \equiv \ln a. \tag{2}$$

The use of this time parameter for calculating probabilities

[3]Here, and in most of the paper, we assume an irreducible landscape, where any metastable inflating vacuum is accessible from any other such vacuum through a sequence of transitions. Alternatively, if the landscape splits into several disconnected sectors, each sector will be characterized by an independent probability distribution and our discussion will still be applicable to any of these sectors. The distribution in case of a reducible landscape is discussed in Appendix A.

is advocated in Ref. [37] and is studied in various contexts in Refs. [6,8–10].[4] It amounts to measuring time in units of the local Hubble time H^{-1},

$$dt = Hd\tau. \tag{3}$$

The scale-factor cutoff is imposed at a fixed value of $t = t_c$, or, equivalently, at a fixed expansion factor a_c.

The term "scale factor" is often used in the context of homogeneous and isotropic spaces, but it is easily generalized to spacetimes with no such symmetry. In the general case, the scale-factor time can be defined by Eq. (3) with

$$H = (1/3)u^{\mu}{}_{;\mu}, \tag{4}$$

where $u^{\mu}(x)$ is the four-velocity vector along the geodesics. This definition has a simple geometric meaning, which can be seen by imagining that the congruence of geodesics describes the flow of a "dust" of test particles. If the dust of particles is assumed to have a uniform density ρ_0 on the initial surface Σ, then the four-current of the dust can be described by $j^{\mu}(x) = \rho(x)u^{\mu}(x)$, where $\rho = \rho_0$ on Σ. Conservation of the current then implies that $u^{\mu}\partial_{\mu}\rho + \rho u^{\mu}{}_{;\mu} = 0$, which with Eqs. (3) and (4) implies that

$$D_{\tau}\ln\rho = -u^{\mu}{}_{;\mu} = -3D_{\tau}t, \tag{5}$$

where $D_{\tau} \equiv u^{\mu}\partial_{\mu}$ is the derivative with respect to proper time along the geodesics. The solution is then $\rho = \rho_0 e^{-3t}$. From Eq. (2) we then have $a \propto \rho^{-1/3}$, so the scale-factor cutoff is triggered when the density $\rho(x)$ of the dust in its own rest frame drops below a certain specified level.

The divergence of geodesics during inflation or homogeneous expansion can be followed by convergence during structure formation or in regions dominated by a negative cosmological constant. The scale-factor time then ceases to be a good time variable, but this does not preclude one from using it to impose a cutoff. A geodesic is terminated when the scale factor first reaches the cutoff value a_c. If the scale factor turns around and starts decreasing before reaching that value, we continue the geodesic all the way to the crunch. When geodesics cross we can still define the scale-factor time along each geodesic according to Eqs. (3) and (4); then one includes a point in $\Gamma(\Sigma, t_c)$ if it lies on any geodesic prior to the first occurrence of $t = t_c$ on that geodesic.

To facilitate further discussion, it will be useful to review some general features of eternally inflating spacetimes, and how they are reflected in proper time and scale-factor time slicings. Regions of an eternally inflating multiverse may evolve in two distinct ways. In the case of quantum diffusion [38,39], inflation is driven by the potential energy of some light scalar fields, the evolution of which is dominated by quantum fluctuations and is described by the Fokker-Planck equation (see e.g. Ref. [10]). Pockets form when the scalar field(s) fluctuate into a region of parameter space where classical evolution dominates, and slow-roll inflation ensues. One can define spacelike hypersurfaces separating the quantum and classical regimes (see, for example, Ref. [15]), which we denote by Σ_q. In universes like ours, slow-roll inflation is followed by thermalization (reheating) and the standard post-inflationary evolution. We denote the hypersurface of thermalization, which separates the inflationary and post-inflationary epochs, as Σ_*.

The multiverse may also (or instead) feature massive fields associated with large false-vacuum energies. Evolution is then governed by bubble nucleation through quantum tunneling [40,41] and can be described to good approximation by a suitable master equation [15,42]. The tunneling may proceed into another local minimum, into a region of quantum diffusion, or into a region of classical slow-roll inflation. In the latter case, the bubble interiors have the geometry of open Friedmann-Robertson-Walker (FRW) universes [43]. Bubbles of interest to us here have a period of slow-roll inflation followed by thermalization. The role of the hypersurface Σ_q is played in this case by the surface separating the initial curvature-dominated regime and the slow-roll regime inside the bubble. The differences between quantum diffusion and tunneling are not important for most of the discussion below, so we shall use notation and terminology interchangeably.

The number of objects of any type that have formed prior to some time t is proportional to $e^{\gamma t}$, where γ is the largest eigenvalue of the physical-volume Fokker-Planck or master equation. This is because the asymptotic behavior is determined by the eigenstate with the largest eigenvalue. Similarly, the physical volume that thermalizes into pockets of type j between times t and $t + dt$ has the form

$$dV_{*j} = C_j e^{\gamma t} dt, \tag{6}$$

where C_j is a constant that depends on the type of pocket. (This was derived in Ref. [6] for models with quantum diffusion and in Refs. [22,44] for models with bubble nucleation.)

The value of γ in Eq. (6) is the same for all pockets, but it depends on the choice of time variable t. With a proper-time slicing, it is given by

$$\gamma \sim 3H_{\max} \qquad (t = \tau), \tag{7}$$

where $H_{\max}$ is the expansion rate of the highest-energy vacuum in the landscape, and corrections associated with decay rates and upward tunneling rates have been ignored. In this case the overall expansion of the multiverse is driven by this fastest-expanding vacuum, which then "trickles down" to all of the other vacua. With scale-factor

[4]The measure studied in Ref. [37] is a comoving-volume measure on surfaces of constant scale-factor time; it is different from the scale-factor cutoff measure being discussed here. In particular, the former measure has a strong dependence on the initial state at the hypersurface Σ. Our measure is very similar to one studied in Ref. [8], which is called the "pseudo-comoving volume-weighted measure."

slicing, all regions would expand as $a^3 = e^{3t}$ if it were not for the continuous loss of volume to terminal vacua with negative or zero Λ. Because of this loss, the value of γ is slightly smaller than 3, and the difference is determined mostly by the rate of decay of the slowest-decaying (dominant) vacuum in the landscape [45],

$$\gamma \approx 3 - \kappa_D \qquad (t = \ln a). \tag{8}$$

Here,

$$\kappa_D = (4\pi/3)\Gamma_D/H_D^4, \tag{9}$$

where Γ_D is the decay rate of the dominant vacuum per unit spacetime volume, and H_D is its expansion rate. The vacuum decay rate is typically exponentially suppressed, so for the slowest-decaying vacuum we expect it to be extremely small. Hence,

$$3 - \gamma \ll 1. \tag{10}$$

B. The youngness bias

As we have already mentioned, the proper-time cutoff measure leads to rather bizarre predictions, collectively known as the youngness paradox [2,21,22]. With proper-time slicing, Eqs. (6) and (7) tell us that the growth of volume in regions of all types is extremely fast, so at any time the thermalized volume is exponentially dominated by regions that have just thermalized. With this superfast expansion, observers who take a little less time to evolve are rewarded by a huge volume factor. This means most observers form closer to the cutoff, when there is much more volume available. Assuming that $H_{\max}$ is comparable to the Planck scale, as one might expect in the string theory landscape, then observers who evolved faster than us by $\Delta\tau = 10^9$ years would have an available thermalized volume which is larger than the volume available to us by a factor of

$$e^{\gamma\Delta\tau} \sim e^{3H_{\max}\Delta\tau} \sim \exp(10^{60}). \tag{11}$$

Unless the probability of life evolving so fast is suppressed by a factor greater than $\exp(10^{60})$, then these rapidly evolving observers would outnumber us by a huge factor. Since these observers would measure the cosmic microwave background (CMB) temperature to be $T = 2.9$ K, it would be hard to explain why we measure it to be $T = 2.73$ K. Note that because $H_{\max}\Delta\tau$ appears in the exponent, the situation is qualitatively unchanged by considering much smaller values of $H_{\max}$ or $\Delta\tau$.

The situation with a scale-factor cutoff is very different. To illustrate methods used throughout this paper, let us be more precise. Let Δt denote the interval in scale-factor time between the time of thermalization, t_*, and the time when some class of observers measures the CMB temperature. A time cutoff excludes the counting of observers who measure the CMB temperature at times later than t_c, so the number of counted observers is proportional to the total volume V_* that thermalizes at any time $t_* < t_c - \Delta t$. (The volume of each region contributing to V_* is measured at the time of its thermalization. For simplicity we focus on pockets that have the same low-energy physics as ours.) The volume of regions thermalized per unit time is given by Eq. (6). A tiny fraction of this volume may decay by tunneling transitions during the subsequent time interval Δt, but we will ignore this effect. For a given Δt, the volume that thermalizes before $t_c - \Delta t$, as counted by the scale-factor cutoff measure, is

$$V_*(\Delta t) \propto \int_{-\infty}^{t_c-\Delta t} e^{\gamma t_*} dt_* \propto e^{-\gamma\Delta t}. \tag{12}$$

To compare with the results above, consider the relative amounts of volume (measure at thermalization) available for the subsequent evolution of two different civilizations, which form at two different time intervals since thermalization, Δt_1 and Δt_2:

$$\frac{V_*(\Delta t_1)}{V_*(\Delta t_2)} = e^{\gamma(\Delta t_2 - \Delta t_1)} = (a_2/a_1)^\gamma, \tag{13}$$

where a_i is the scale factor at time $t_* + \Delta t_i$. Thus, taking $\gamma \approx 3$, the relative volumes available for observers who measure the CMB at the present value ($T = 2.73$ K), compared to observers who measure it at the value of 10^9 years ago ($T = 2.9$ K), is given by

$$\frac{V_*(2.73\ \text{K})}{V_*(2.9\ \text{K})} \approx \left(\frac{2.73\ \text{K}}{2.9\ \text{K}}\right)^3 \approx 0.8. \tag{14}$$

Thus, the youngness bias is very mild in the scale-factor cutoff measure. Yet, as we shall see, it can have interesting observational implications.

C. Expectations for the density contrast Q and the density parameter Ω

Pocket-based measures, as well as "gauge-invariant" measures, suffer from a "Q catastrophe" where one expects to measure extreme values of the primordial density contrast Q. To see this, note that these measures exponentially prefer parameter values that generate a large number of e-folds of inflation. This by itself does not appear to be a problem, but Q is related to parameters that determine the number of e-folds. The result of this is a selection effect that exponentially prefers the observation of either very large or very small values of Q, depending on the model of inflation and on which inflationary parameters scan (i.e., which parameters vary significantly across the landscape) [23,24]. On the other hand, we observe Q to lie comfortably in the middle of the anthropic range [46], indicating that no such strong selection effect is at work.[5] Note that a similar story applies to the magnitude of the gravitational constant G [25].

[5]Possible resolutions to this problem have been proposed in Refs. [23,24,47,48].

With the scale-factor cutoff, on the other hand, this is not a problem. To see this, consider a landscape in which the only parameter that scans is the number of e-folds of inflation; all low-energy physics is exactly as in our Universe. Consider first the portions of the hypersurfaces Σ_q that begin slow-roll inflation at time t_q in the interval dt_q. These regions begin with a physical volume proportional to $e^{\gamma t_q} dt_q$, and those that do not decay grow by a factor of e^{3N_e} before they thermalize at time $t_* = t_q + N_e$. If κ_I is the transition rate out of the slow-roll inflationary phase [as defined in Eq. (9)], then the fraction of volume that does not undergo decay is $e^{-\kappa_I N_e}$.

After thermalization at time t_*, the evolution is the same in all thermalized regions. Therefore we ignore this common evolution and consider the number of observers measuring a given value of N_e to be proportional to the volume of thermalization hypersurfaces that appear at times earlier than the cutoff at scale-factor time t_c. This cutoff requires $t_* = t_q + N_e < t_c$. Summing over all times t_q gives

$$P(N_e) \propto e^{(3-\kappa_I)N_e} \int_{-\infty}^{t_c - N_e} e^{\gamma t_q} dt_q \propto e^{(3-\gamma-\kappa_I)N_e}. \quad (15)$$

Even though the dependence on N_e is exponential, the factor

$$3 - \gamma - \kappa_I \approx \kappa_D - \kappa_I \quad (16)$$

is exponentially suppressed. Thus we find $P(N_e)$ is a very weak function of N_e, and there is not a strong selection effect for a large number of e-folds of slow-roll inflation. In fact, since the dominant vacuum D is by definition the slowest-decaying vacuum, we have $\kappa_I > \kappa_D$. Thus the scale-factor cutoff introduces a very weak selection for smaller values of N_e.[6]

Because of the very mild dependence on N_e, we do not expect the scale-factor measure to impose significant cosmological selection on the scanning of any inflationary parameters. Thus, there is no Q catastrophe—nor is there the related problem for G—and the distribution of Q is essentially its distribution over the states in the landscape, modulated by inflationary dynamics and any anthropic selection effects.

The distribution $P(N_e)$ is also important for the expected value of the density parameter Ω. This is because the deviation of Ω from unity decreases during an inflationary era,

$$|\Omega - 1| \propto e^{-2N_e}. \quad (17)$$

Hence pocket-based and "gauge-invariant" measures, which exponentially favor large values of N_e, predict a universe with Ω extremely close to unity. The distributions of Ω from a variety of models have been calculated using a pocket-based measure in Refs. [13,44].

On the other hand, as we have just described, the scale-factor cutoff measure does not significantly select for any value of N_e. There will still be some prior distribution of N_e, related to the distributions of inflationary parameters over the states in the landscape, but it is not necessary that N_e be driven strongly toward large values (in fact, it has been argued that small values should be preferred in the string landscape, see e.g. Ref. [49]). Thus, it appears that the scale-factor cutoff allows for the possibility of a detectable negative curvature. The probability distribution of Ω in this type of measure has been discussed qualitatively in Ref. [49]; a more detailed quantitative analysis will be given elsewhere [50].

III. THE DISTRIBUTION OF Λ

A. Model assumptions

We now consider a landscape of vacua with the same low-energy physics as we observe, except for an essentially continuous distribution of possible values of Λ. According to Eq. (6), the volume that thermalizes between times t_* and $t_* + dt_*$ with values of cosmological constant between Λ and $\Lambda + d\Lambda$ is given by

$$dV_*(\Lambda) = C(\Lambda) d\Lambda e^{\gamma t_*} dt_*. \quad (18)$$

The factor of $C(\Lambda)$ plays the role of the "prior" distribution of Λ; it depends on the spectrum of possible values of Λ in the landscape and on the dynamics of eternal inflation. The standard argument [26,29] suggests that $C(\Lambda)$ is well approximated by

$$C(\Lambda) \approx \text{const}, \quad (19)$$

because anthropic selection restricts Λ to values that are very small compared to its expected range of variation in the landscape. The conditions of validity of this heuristic argument have been studied in simple landscape models [45,51,52], with the conclusion that it does in fact apply to a wide class of models. Here, we shall assume that Eq. (19) is valid.

Anthropic selection effects are usually characterized by the fraction of matter that has clustered in galaxies. The idea here is that a certain average number of stars is formed per unit galactic mass and a certain number of observers per star, and that these numbers are not strongly affected by the value of Λ. Furthermore, the standard approach is to assume that some minimum halo mass M_G is necessary to drive efficient star formation and heavy element retention. Since we regulate the volume of the multiverse using a time cutoff, it is important for us to also track at what time observers arise. We assume that after halo collapse, some fixed proper time lapse $\Delta\tau$ is required to allow for stellar, planetary, and biological evolution before an observer can measure Λ. Then the number of observers measuring Λ before some time τ in a thermalized volume of size V_* is

[6]We are grateful to Ben Freivogel for pointing out to us the need to account for vacuum decay during slow-roll inflation. He has also suggested that this effect will lead to preference for smaller values of N_e.

roughly

$$\mathcal{N} \propto F(M_G, \tau - \Delta\tau)V_*, \tag{20}$$

where F is the collapse fraction, measuring the fraction of matter that clusters into objects of mass greater than or equal to M_G, at time $\tau - \Delta\tau$.

Anthropic selection for structure formation ensures that within each relevant pocket matter dominates the energy density before Λ does. Thus, all thermalized regions evolve in the same way until well into the era of matter domination. To draw upon this common evolution, within each pocket we define proper time τ with respect to a fixed time of thermalization, τ_*. It is convenient to also define a reference time τ_m such that τ_m is much larger than the time of matter-radiation equality and much less than the time of matter-Λ equality. Then evolution before time τ_m is the same in every pocket, while after τ_m the scale factor evolves as

$$\tilde{a}(\tau) = \begin{cases} H_\Lambda^{-2/3}\sinh^{2/3}(\frac{3}{2}H_\Lambda\tau) & \text{for } \Lambda > 0 \\ H_\Lambda^{-2/3}\sin^{2/3}(\frac{3}{2}H_\Lambda\tau) & \text{for } \Lambda < 0. \end{cases} \tag{21}$$

Here we have defined

$$H_\Lambda \equiv \sqrt{|\Lambda|/3}, \tag{22}$$

and use units with $G = c = 1$. The prefactors $H_\Lambda^{-2/3}$ ensure that early evolution is identical in all thermalized regions. This means the global scale factor a is related to $\tilde{a}$ by some factor that depends on the scale-factor time t_* at which the region of interest thermalized.

In the case $\Lambda > 0$, the rate at which halos accrete matter decreases with time and halos may settle into galaxies that permit quiescent stellar systems such as ours. The situation with $\Lambda < 0$ is quite different. At early times, the evolution of overdensities is the same; but when the proper time reaches $\tau_{\rm turn} = \pi/3H_\Lambda$, the scale factor begins to decrease and halos begin to accrete matter at a rate that increases with time. Such rapid accretion may prevent galaxies from settling into stable configurations, which in turn would cause planetary systems to undergo more frequent close encounters with passing stars. This effect might become significant even before turnaround, since our present environment benefits from positive Λ slowing the collision rate of the Milky Way with other systems.

For this reason, we use Eq. (20) to estimate the number of observers if $\Lambda > 0$, but for $\Lambda < 0$ we consider two alternative anthropic hypotheses:

(A) we use Eq. (20), but of course taking account of the fact that the proper time τ cannot exceed $\tau_{\rm crunch} = 2\pi/3H_\Lambda$; or

(B) we use Eq. (20), but with the hypothesis that the proper time τ is capped at $\tau_{\rm turn} = \pi/3H_\Lambda$.

Here $\tau_{\rm crunch}$ refers to the proper time at which a thermalized region in a collapsing pocket reaches its future singularity, which we refer to as its "crunch." Anthropic hypothesis A corresponds to the assumption that life can form in any sufficiently massive collapsed halo, while anthropic hypothesis B reflects the assumption that the probability for the formation of life becomes negligible in the tumultuous environment following turnaround. Similar hypotheses for $\Lambda < 0$ were previously used in Ref. [34]. It seems reasonable to believe that the truth lies somewhere between these two hypotheses, perhaps somewhat closer to hypothesis B.

B. Distribution of Λ using a pocket-based measure

Before calculating the distribution of Λ using a scale-factor cutoff, we review the standard calculation [29–34]. This approach assumes an ensemble of equal-size regions with a flat prior distribution of Λ. The regions are allowed to evolve indefinitely, without any time cutoff, so in the case of $\Lambda > 0$ the selection factor is given by the asymptotic collapse fraction at $\tau \to \infty$. For $\Lambda < 0$ we shall consider anthropic hypotheses A and B. This prescription corresponds to using the pocket-based measure, in which the ensemble includes spherical regions belonging to different pockets and observations are counted in the entire comoving history of these regions. The corresponding distribution function is given by

$$P(\Lambda) \propto \begin{cases} F(M_G, \tau \to \infty) & \text{for } \Lambda > 0 \\ F(M_G, \tau_{\rm crunch} - \Delta\tau) & \text{for } \Lambda < 0 (A) \\ F(M_G, \tau_{\rm turn} - \Delta\tau) & \text{for } \Lambda < 0 (B), \end{cases} \tag{23}$$

where, again, $\tau_{\rm crunch} = 2\pi/3H_\Lambda$ is the proper time of the crunch in pockets with $\Lambda < 0$, while $\tau_{\rm turn} = \pi/3H_\Lambda$.

We approximate the collapse fraction F using the Press-Schechter (PS) formalism [53], which gives

$$F(M_G, \tau) = \text{erfc}\left[\frac{\delta_c(\tau)}{\sqrt{2}\sigma(M_G, \tau)}\right], \tag{24}$$

where $\sigma(M_G, \tau)$ is the root-mean-square fractional density contrast $\delta M/M$ averaged over a comoving scale enclosing mass M_G and evaluated at proper time τ, while δ_c is the collapse density threshold. As is further explained in Appendix B, $\delta_c(\tau)$ is determined by considering a "top-hat" density perturbation in a flat universe, with an arbitrary initial amplitude. $\delta_c(\tau)$ is then defined as the amplitude reached by the linear evolution of an overdensity of nonrelativistic matter $\delta\rho_m/\rho_m$ that has the same initial amplitude as a top-hat density perturbation that collapses to a singularity in proper time τ. $\delta_c(\tau)$ has the constant value of 1.686 in an Einstein-de Sitter universe (i.e., flat, matter-dominated universe), but it evolves with time when $\Lambda \neq 0$ [54,55]. We simulate this evolution using the fitting functions (B23), which are accurate to better than 0.2%. Note, however, that the results do not change by more than a few percent if one simply uses the constant value $\delta_c = 1.686$.

Aside from providing the collapse fraction, the PS formalism describes the "mass function," i.e. the distribution of halo masses as a function of time. N-body simulations indicate that PS model overestimates the abundance of halos near the peak of the mass function, while underestimating that of more massive structures [56]. Consequently, other models have been developed (see e.g. Refs. [57]), while others have studied numerical fits to N-body results [34,58]. From each of these approaches, the collapse fraction can be obtained by integrating the mass function. We have checked that our results are not significantly different if we use the fitting formula of Ref. [34] instead of Eq. (24). Meanwhile, we prefer Eq. (24) to the fit of Ref. [34] because the latter was performed using only numerical simulations with $\Lambda > 0$.

The evolution of the density contrast σ is treated linearly, to be consistent with the definition of the collapse density threshold δ_c. Thus we can factorize the behavior of $\sigma(M_G, \tau)$, writing

$$\sigma(M_G, \tau) = \bar{\sigma}(M_G) G_\Lambda(\tau), \tag{25}$$

where $G_\Lambda(\tau)$ is the linear growth function, which is normalized so that the behavior for small τ is given by $G_\Lambda(\tau) \sim (3H_\Lambda \tau/2)^{2/3}$. In Appendix B we will give exact integral expressions for $G_\Lambda(\tau)$, and also the fitting formulae (B12) and (B13), taken from Ref. [34], that we actually used in our calculations. Note that for $\Lambda \geq 0$ the growth rate $\dot{G}_\Lambda(\tau)$ always decreases with time [$\ddot{G}_\Lambda(\tau) < 0$], while for $\Lambda < 0$ the growth rate reaches a minimum at $\tau \approx 0.24\tau_{\rm crunch}$ and then starts to accelerate. This accelerating rate of growth is related to the increasing rate of matter accretion in collapsed halos after turnaround, which we mentioned above in motivating the anthropic hypothesis B.

The prefactor $\bar{\sigma}(M_G)$ in Eq. (25) depends on the scale M_G at which the density contrast is evaluated. According to our anthropic model, M_G should correspond to the minimum halo mass for which star formation and heavy element retention is efficient. Indeed, the efficiency of star formation is seen to show a sharp transition: it falls abruptly for halo masses smaller than $M_G \sim 2 \times 10^{11} M_\odot$, where $M_\odot$ is the solar mass [59]. Peacock [34] showed that the existing data on the evolving stellar density can be well described by a Press-Schechter calculation of the collapsed density for a single mass scale, with a best fit corresponding to $\sigma(M_G, \tau_{1000}) \approx 6.74 \times 10^{-3}$, where τ_{1000} is the proper time corresponding to a temperature $T = 1000$ K. Using cosmological parameters current at the time, Peacock found that this perturbation amplitude corresponds to an effective galaxy mass of $1.9 \times 10^{12} M_\odot$. Using the more recent WMAP-5 parameters [60], as is done throughout this paper,[7] we find (using Ref. [61] and the CMBFAST program) that the corresponding effective galaxy mass is $1.8 \times 10^{12} M_\odot$.

Unless otherwise noted, in this paper we set the prefactor $\bar{\sigma}(M_G)$ in Eq. (25) by choosing $M_G = 10^{12} M_\odot$. Using the WMAP-5 parameters and CMBFAST, we find that at the present cosmic time $\sigma(10^{12} M_\odot) \approx 2.03$. This corresponds to $\sigma(10^{12} M_\odot, \tau_{1000}) \approx 7.35 \times 10^{-3}$.

We are now prepared to display the results, plotting $P(\Lambda)$ as determined by Eq. (23). We first reproduce the standard distribution of Λ, which corresponds to the case when $\Lambda > 0$. This is shown in Fig. 1. We see that the value of Λ that we measure is between one and two standard deviations from the mean. Throughout the paper, the vertical bars in the plots merely highlight the observed value of Λ and do not indicate its experimental uncertainty. The quality of the fit depends on the choice of scale M_G; in particular, choosing smaller values of M_G weakens the fit [33,62]. Note, however, that the value of M_G that we use is already less than that recommended by Ref. [34].

Figure 2 shows the distribution of Λ for positive and negative values of Λ. We use $\Delta\tau = 5 \times 10^9$ years, corresponding roughly to the age of our solar system. The left column corresponds to choosing anthropic hypothesis A while the right column corresponds to anthropic hypothesis B. To address the question of whether the observed value of $|\Lambda|$ lies improbably close to the special point $\Lambda = 0$, in the second row we plot the distributions for $P(|\Lambda|)$. We see that the observed value of Λ lies only a little more than 1 standard deviation from the mean, which is certainly acceptable. (Another measure of the "typicality" of our value of Λ has been studied in Ref. [33]).

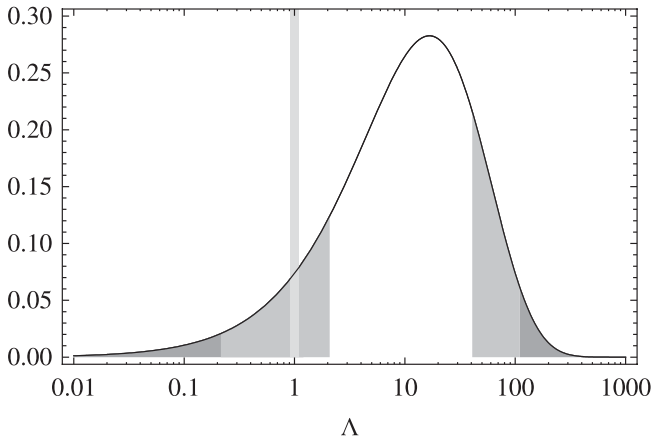

FIG. 1. The normalized distribution of Λ for $\Lambda > 0$, with Λ in units of the observed value, for the pocket-based measure. The vertical bar highlights the value we measure, while the shaded regions correspond to points more than one and two standard deviations from the mean. Here and in subsequent graphs with logarithmic abscissas, the vertical axis shows the probability density per e-fold, $\Lambda P(\Lambda)$.

[7]The relevant values are $\Omega_\Lambda = 0.742$, $\Omega_m = 0.258$, $\Omega_b = 0.044$, $n_s = 0.96$, $h = 0.719$, and $\Delta^2_{\mathcal{R}}(k = 0.02\ \mathrm{Mpc}^{-1}) = 2.21 \times 10^{-9}$.

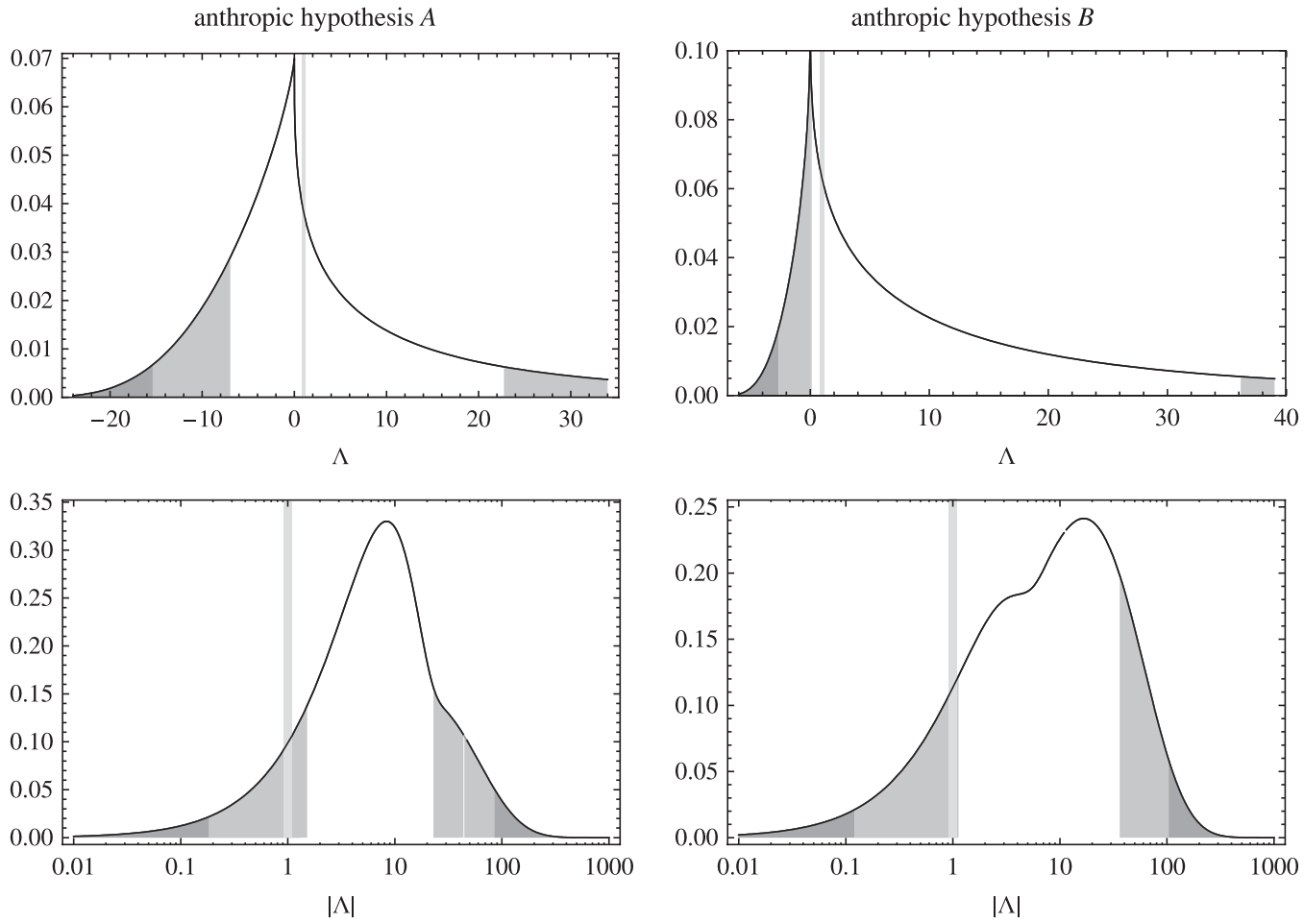

FIG. 2. The normalized distribution of Λ, with Λ in units of the observed value, for the pocket-based measure. The left column corresponds to anthropic hypothesis A while the right column corresponds to anthropic hypothesis B. Meanwhile, the top row shows $P(\Lambda)$ while the bottom row shows $|\Lambda|P(|\Lambda|)$. The vertical bars highlight the value we measure, while the shaded regions correspond to points more than one and two standard deviations from the mean.

C. Distribution of Λ using the scale-factor cutoff

We now turn to the calculation of $P(\Lambda)$ using a scale-factor cutoff to regulate the diverging volume of the multiverse. When we restrict attention to the evolution of a small thermalized patch, a cutoff at scale-factor time t_c corresponds to a proper-time cutoff τ_c, which depends on t_c and the time at which the patch thermalized, t_*. Here we take the thermalized patch to be small enough that scale-factor time t is essentially constant over hypersurfaces of constant τ. Then the various proper and scale-factor times are related by

$$t_c - t_* = \int_{\tau_*}^{\tau_c} H(\tau) d\tau = \ln[\tilde{a}(\tau_c)/\tilde{a}(\tau_*)]. \tag{26}$$

Recall that all of the thermalized regions of interest share a common evolution up to the proper time τ_m, after which they follow Eqs. (21). Solving for the proper-time cutoff τ_c gives

$$\tau_c = \tfrac{2}{3} H_\Lambda^{-1} \operatorname{arcsinh}[\tfrac{3}{2} H_\Lambda \tau_m e^{3/2(t_c - t_* - C)}], \tag{27}$$

for the case $\Lambda > 0$, and

$$\tau_c = \tfrac{2}{3} H_\Lambda^{-1} \arcsin[\tfrac{3}{2} H_\Lambda \tau_m e^{(3/2)(t_c - t_* - C)}], \tag{28}$$

for $\Lambda < 0$. The term $C = \frac{2}{3} \ln(\tau_m/\tau_*)$ is a constant that accounts for evolution from time τ_* to time τ_m. Note that as $t_c - t_*$ is increased in Eq. (28), τ_c grows until it reaches the time of scale-factor turnaround in the pocket, $\tau_{\text{turn}} = \pi/3H_\Lambda$, after which the expression is ill defined. Physically, the failure of Eq. (28) corresponds to when a thermalized region reaches turnaround before the scale-factor time reaches its cutoff at t_c. After turnaround, the scale factor decreases; therefore these regions evolve without a cutoff all the way up to the time of crunch, $\tau_{\text{crunch}} = 2\pi/3H_\Lambda$.

When counting the number of observers in the various pockets using a scale-factor cutoff, one must keep in mind the dependence on the thermalized volume V_* in Eq. (20),

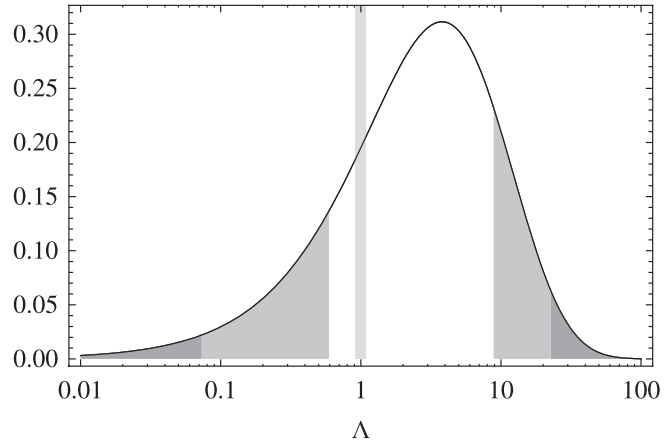

FIG. 3. The normalized distribution of Λ for $\Lambda > 0$, with Λ in units of the observed value, for the scale-factor cutoff. The vertical bar highlights the value we measure, while the shaded regions correspond to points more than one and two standard deviations from the mean.

since in this case V_* depends on the cutoff. As stated earlier, we assume the rate of thermalization for pockets containing universes like ours is independent of Λ. Thus, the total physical volume of all regions that thermalized between times t_* and $t_* + dt_*$ is given by Eq. (6), and is independent of Λ. Using Eq. (20) to count the number of observers in each thermalized patch, and summing over all times below the cutoff, we find

$$P(\Lambda) \propto \int_{-\infty}^{t_c} F[M_G, \tau_c(t_c, t_*) - \Delta\tau] e^{\gamma t_*} dt_*. \tag{29}$$

Note that regions thermalizing at a later time t_* have a greater weight $\propto e^{\gamma t_*}$. This is an expression of the youngness bias in the scale-factor measure. The Λ dependence of this distribution is implicit in F, which depends on $\delta_c(\Lambda, \tau_c - \Delta\tau)/\sigma_{\rm rms}(\Lambda, \tau_c - \Delta\tau)$, and in turn on $\tau_c(\Lambda)$, which is described below.

For pockets with $\Lambda > 0$, the cutoff on proper time τ_c is given by Eqs. (27) and (28). Meanwhile, when $\Lambda < 0$, τ_c is

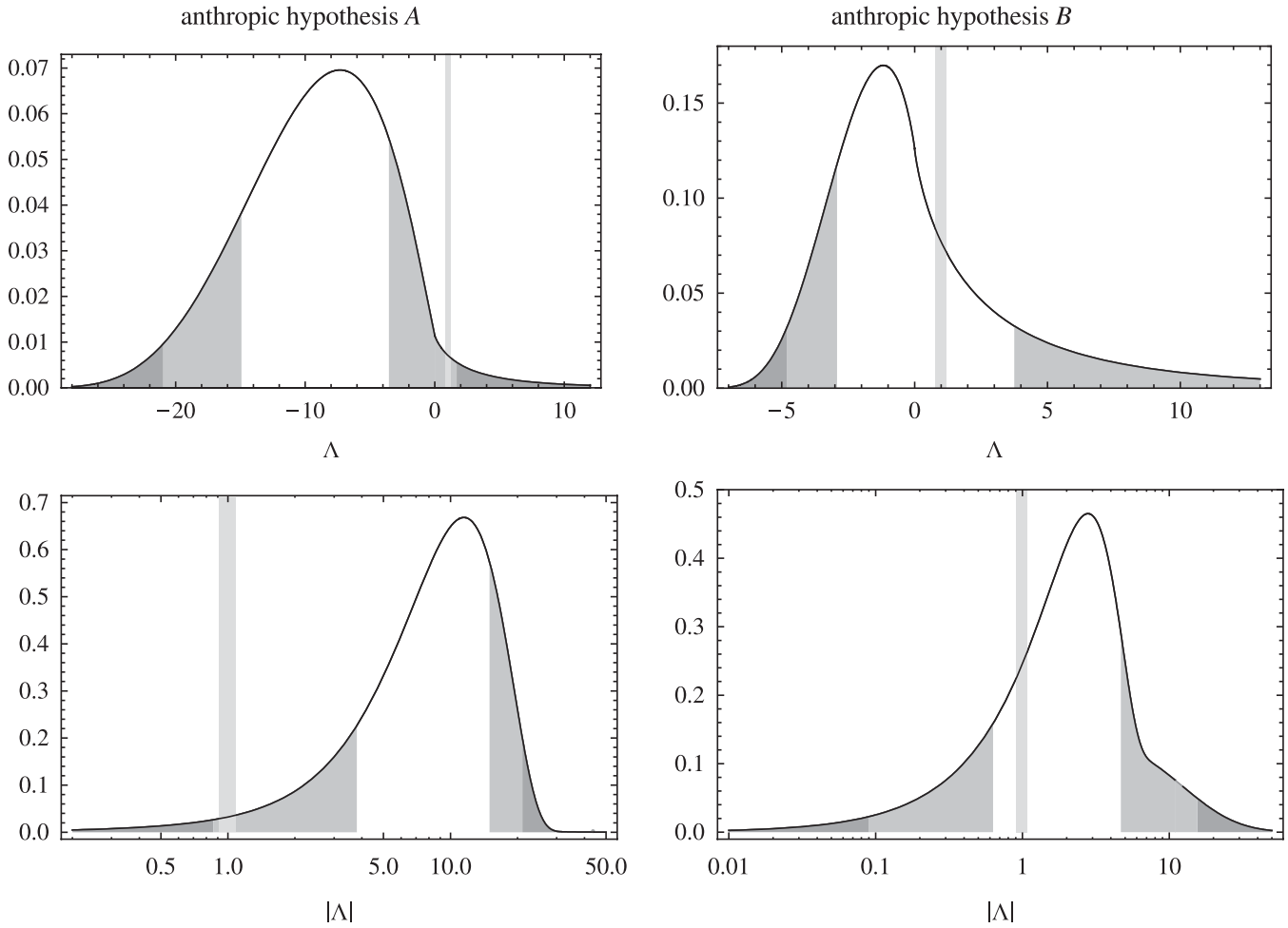

FIG. 4. The normalized distribution of Λ, with Λ in units of the observed value, for the scale-factor cutoff. The left column corresponds to anthropic hypothesis A while the right column corresponds to anthropic hypothesis B. Meanwhile, the top row shows $P(\Lambda)$ while the bottom row shows $|\Lambda|P(|\Lambda|)$. The vertical bars highlight the value we measure, while the shaded regions correspond to points more than one and two standard deviations from the mean.

given by Eq. (28), when that expression is well defined. In practice, the constant C of Eqs. (27) and (28) is unimportant, since a negligible fraction of structures form before the proper time τ_m. Furthermore, for a reference time τ_m chosen deep in the era of matter domination, the normalized distribution is independent of τ_m. As mentioned above, for sufficiently large $t_c - t_*$ Eq. (28) becomes ill defined, corresponding to the thermalized region reaching its crunch before the scale-factor cutoff. In this case we set $\tau_c = \tau_{\rm crunch}$ or $\tau_c = \tau_{\rm turn}$, corresponding to the anthropic hypothesis A or B described above.

To compare with previous work, we first display the distribution of positive Λ in Fig. 3. We have set $\gamma = 3$ and use $\Delta\tau = 5 \times 10^9$ years. Clearly, the scale-factor cutoff provides an excellent fit to observation, when attention is limited to $\Lambda > 0$. Note that the scale-factor-cutoff distribution exhibits a much faster falloff at large Λ than the pocket-based distribution in Fig. 1. The reason is not difficult to understand. For larger values of Λ, the vacuum energy dominates earlier. The Universe then begins expanding exponentially, and this quickly triggers the scale-factor cutoff. Thus, pockets with larger values of Λ have an earlier cutoff (in terms of the proper time) and have less time to evolve observers. This tendency for the cutoff to kick in soon after Λ-domination may help to sharpen the anthropic explanation [31,63] of the otherwise mysterious fact that we live so close to this very special epoch (matter-Λ equality) in the history of the Universe.

The distribution of Λ for positive and negative values of Λ is displayed in Fig. 4, using the same parameter values as before. We see that the distribution with anthropic hypothesis A provides a reasonable fit to observation, with the measured value of Λ appearing just within two standard deviations of the mean. Note that the weight of this distribution is dominated by negative values of Λ, yet anthropic hypothesis A may not give the most accurate accounting of observers in pockets with $\Lambda < 0$. Anthropic hypothesis B provides an alternative count of the number of observers in regions that crunch before the cutoff, and we see that the corresponding distributions provide a very good fit to observation. This is the main result of this work.

The above distributions all use $\Delta\tau = 5 \times 10^9$ years and $M_G = 10^{12} M_\odot$. These values are motivated, respectively, by the age of our solar system and by the mass of our galactic halo, the latter being a good match to an empirical fit determining the halo mass scale characterizing efficient star formation [34]. Yet, to illustrate the dependence of our main result on $\Delta\tau$ and M_G, in Fig. 5 we display curves for anthropic hypothesis B, using $\Delta\tau = 3$, 5, and 7×10^9 years and using $M_G = 10^{10}$, 10^{11}, and $10^{12} M_\odot$. The distribution varies significantly as a result of these changes, but the fit to the observed value of Λ remains good.

IV. CONCLUSIONS

To date, several qualitatively distinct measures have been proposed to regulate the diverging volume of the multiverse. Although theoretical analysis has not provided much guidance as to which of these, if any, is correct, the various regulating procedures make different predictions for the distributions of physical observables. Therefore, one can take an empirical approach, comparing the predictions of various measures to our observations, to shed light on what measures are on the right track. With this in mind, we have studied some aspects of a scale-factor cutoff measure. This measure averages over the spacetime volume in a comoving region between some initial spacelike hypersurface Σ and a final hypersurface of constant time, with time measured in units of the local Hubble rate along the comoving geodesics. At the end of the calculation, the

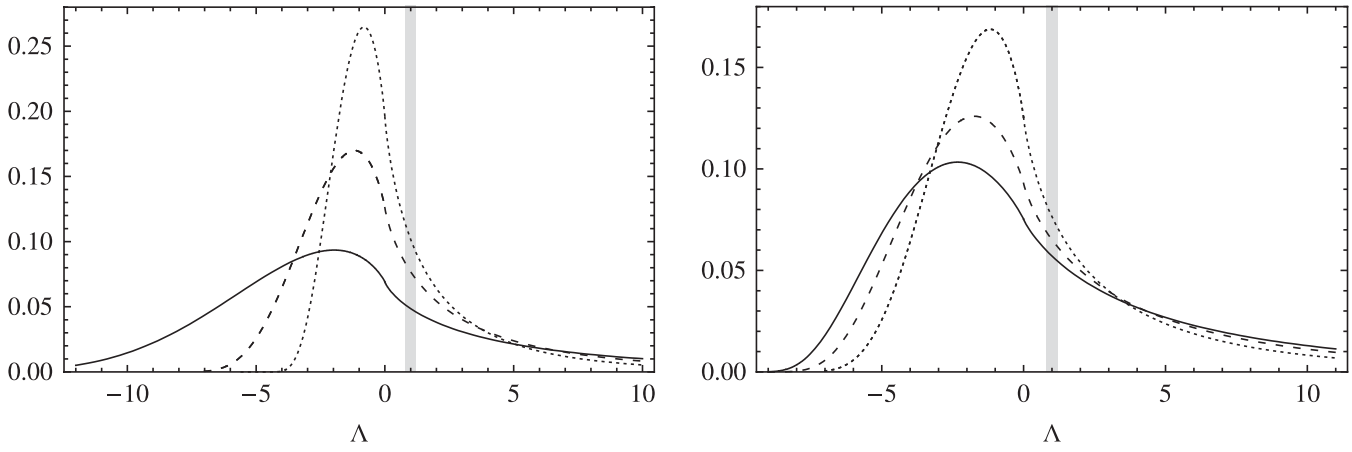

FIG. 5. The normalized distribution of Λ, with Λ in units of the observed value, for anthropic hypothesis B in the scale-factor cutoff. The left panel displays curves for $\Delta\tau = 3$ (solid line), 5 (dashed line), and 7(dotted) $\times 10^9$ years, with $M_G = 10^{12} M_\odot$, while the right panel displays curves for $M_G = 10^{10} M_\odot$ (solid line), $10^{11} M_\odot$ (dashed line), and $10^{12} M_\odot$ (dotted line), with $\Delta\tau = 5 \times 10^9$ years. The vertical bars highlight the value of Λ that we measure.

cutoff on scale-factor time is taken to infinity. We shall now summarize what we have learned about the scale-factor measure and compare its properties to those of other proposed measures.

The "empirical approach" that we follow focuses attention on measures that avoid basic conflicts between prediction and observation. The most severe of these conflicts is the "youngness paradox"—the prediction of an extremely youth-dominated distribution of observers—which follows from the proper-time cutoff measure. The scale-factor cutoff measure, on the other hand, predicts only a very mild youngness bias, which is consistent with observation. Another problem, which arises in pocket-based and "gauge-invariant" measures, is the Q catastrophe, where one expects to measure the amplitude of the primordial density contrast Q to have an unfavorably large or small value. This problem ultimately stems from an exponential preference for a large number of e-folds of slow-roll inflation in these measures. The scale-factor cutoff does not strongly select for more inflation, and thus does not suffer from a Q catastrophe. An unattractive feature of causal-patch and comoving-volume measures is that their predictions are sensitive to the assumptions one makes about the initial conditions for the multiverse. In contrast, the scale-factor cutoff measure is essentially independent of the initial state. This property reflects the attractor character of eternal inflation: the asymptotic late-time evolution of an eternally inflating universe is independent of the starting point.

With any measure over the multiverse, one must *also* be wary that it does not overpredict "Boltzmann brains"—observers that pop in and out of existence as a result of rare quantum fluctuations [64]. This issue has not been addressed here, but our preliminary analysis suggests that, with some assumptions about the landscape, the scale-factor cutoff measure does not have a Boltzmann brain problem. We shall return to this issue in a separate publication [65].

As mentioned above, a key feature of the scale-factor cutoff measure is that, unlike the pocket-based or "gauge-invariant" measures, it does not reward large amounts of slow-roll inflation. As a result, it allows for the possibility of a detectable negative curvature. This issue will be discussed in detail in Ref. [50].

The main focus of this paper has been on the probability distribution for the cosmological constant Λ. Although the statistical distribution of Λ among states in the landscape is assumed to be flat, imposing a scale-factor cutoff modulates this distribution to prefer smaller values of Λ. Combined with appropriate anthropic selection effects, this gives a distribution of Λ that is in a good fit with observation. We have calculated the distribution for positive and negative values of Λ, as well as for the absolute value $|\Lambda|$. For $\Lambda > 0$, we adopted the standard assumption that the number of observers is proportional to the fraction of matter clustered in halos of mass greater than $10^{12} M_\odot$, and allowed a fixed proper-time interval $\Delta\tau = 5 \times 10^9$ years for the evolution of observers in such halos. For $\Lambda < 0$, we considered two possible scenarios, which probably bracket the range of reasonable possibilities. The first (scenario A) assumes that observations can be made all the way to the big crunch, so we count all halos formed prior to time $\Delta\tau$ before the crunch. The second (scenario B) assumes that the contracting negative-Λ phase is hazardous to life, so we count only halos that formed at time $\Delta\tau$ or earlier before the turnaround.

Our results show that the observed value of Λ is within two standard deviations from the mean for scenario A, and within one standard deviation for scenario B. In the latter case, the fit is better than that obtained in the "standard" calculations [29–34], which assume no time cutoff (this is equivalent to choosing a pocket-based measure on the multiverse). The causal-patch measure also selects for smaller values of Λ providing, in the case of positive Λ, a fit to observation similar to that of the scale-factor cutoff [35]. Note, however, that the approach of Ref. [35] used an entropy-based anthropic weighting (as opposed to the structure-formation-based approach used here) and that the distribution of negative Λ has not been studied in this measure.

We have verified that our results are robust with respect to changing the parameters M_G and $\Delta\tau$. The agreement with the data remains good for M_G varying between 10^{10} and $10^{12} M_\odot$ and for $\Delta\tau$ varying between 3×10^9 and 7×10^9 years. It would be interesting to know how robust these results are with respect to allowing other cosmological parameters to scan along with Λ; we leave this to future work.

ACKNOWLEDGMENTS

We thank Raphael Bousso, Ben Freivogel, Andrei Linde, John Peacock, Delia Schwartz-Perlov, Vitaly Vanchurin, and Serge Winitzki for useful comments and discussions. The work of A. D. S. is supported in part by the INFN. A. D. S. and A. H. G. are supported in part by the U.S. Department of Energy under Contract No. DE-FG02-05ER41360. M. P. S. and A. V. are supported in part by the U.S. National Science Foundation under Grant No. NSF 322.

APPENDIX A: INDEPENDENCE OF THE INITIAL STATE

In Sec. II we assumed that the landscape is irreducible, so that any vacuum is accessible through quantum diffusion or bubble nucleation from any other (de Sitter) vacuum. If instead the landscape splits into several disconnected sectors, the scale-factor cutoff can be used to find the probability distributions $P_j^{(A)}$ in each of the sectors (labeled by A). These distributions are determined

by the dominant eigenstates of the Fokker-Planck or master equation, which correspond to the largest eigenvalues γ_A, and are independent of the choice of the initial hypersurfaces Σ_A that are used in implementing the scale-factor cutoff. But the question still remains, how do we compare the probabilities of vacua belonging to different sectors?

Since different sectors are inaccessible from one another, the probability P_A of being in a given sector must depend on the initial state of the universe. For definiteness, we shall assume here that the initial state is determined by the wave function of the universe, although most of the following discussion should apply to any theory of initial conditions. According to both tunneling [66] and Hartle-Hawking [67] proposals for the wave function, the universe starts as a 3-sphere S_α filled with some positive-energy vacuum α. The radius of the 3-sphere is $r_\alpha = H_\alpha^{-1}$, where H_α is the de Sitter expansion rate. The corresponding nucleation probability is

$$P_{\rm nucl}^{(\alpha)} \propto \exp\left(\pm\frac{\pi}{H_\alpha^2}\right), \tag{A1}$$

where the upper sign is for the Hartle-Hawking and the lower is for the tunneling wave function. Once the universe has nucleated, it immediately enters de Sitter inflationary expansion, transitions from α to other vacua, and populates the entire sector of the landscape to which the vacuum α belongs. We thus have an ensemble of eternally inflating universes with initial conditions at 3-surfaces S_α and the probability distribution $P_{\rm nucl}^{(\alpha)}$ given by Eq. (A1).

If the landscape were not disconnected, we could apply the scale-factor cutoff measure to any single component α of the initial wave function, and the result would be the same in all cases. To generalize the scale-factor cutoff measure to the disconnected landscape, the most straightforward prescription is to apply the scale-factor cutoff directly to the initial probability ensemble. In that case,

$$P_{j,A} \propto \lim_{t_c\to\infty} \sum_{\alpha\in A} P_{\rm nucl}^{(\alpha)} \mathcal{N}_j^{(\alpha)}(t_c). \tag{A2}$$

Here,

$$\mathcal{N}_j^{(\alpha)}(t_c) = R_\alpha^{(A)} P_j^{(A)} e^{\gamma_A t_c} \tag{A3}$$

is the number of relevant observations in the entire closed universe, starting from the hypersurface S_α, with a cutoff at scale-factor time t_c. The $R_\alpha^{(A)}$ are determined by the initial volume of the 3-surface S_α, and also by the efficiency with which this initial state couples to the leading eigenvector of Eq. (6). In other words, the $\mathcal{N}_j^{(\alpha)}(t_c)$ are calculated using S_α as the initial hypersurface Σ_A. Note that only the overall normalization of $\mathcal{N}_j^{(\alpha)}$ depends on the initial vacuum α; the relative probabilities of different vacua in the sector do not. In the limit of $t_c \to \infty$, only the sectors corresponding to the largest of all dominant eigenvalues,

$$\gamma_{\rm max} = \max\{\gamma_A\}, \tag{A4}$$

have a nonzero probability. If there is only one sector with this eigenvalue, this selects the sector uniquely.

Since the issue of initial state dependence is new, one might entertain an alternative method of dealing with the issue, in which the probability P_A for each sector is determined immediately by the initial state, with

$$P_A \propto \sum_{\alpha\in A} P_{\rm nucl}^{(\alpha)}. \tag{A5}$$

Then one could calculate any probability of interest within each sector, using the standard scale-factor cutoff method, and weight the different sectors by P_A. However, although this prescription is well defined, we would advocate the first method that we described as the natural extension of the scale-factor cutoff measure. First, it seems to be more closely related to the description of the scale-factor cutoff measure in a connected landscape: the only change is to replace the initial state by an ensemble of states, determined in principle by one's theory of the initial wave function. Second, in a toy theory, one could imagine approaching a disconnected landscape from a connected one, by gradually decreasing all the cross-sector tunneling rates to zero. In that case, the limit clearly corresponds to the first description, where one sector is selected uniquely if it has the largest dominant eigenvalue.

Assuming the first of these prescriptions, the conclusion is that the probability distribution (A2) defined by the scale-factor measure is essentially independent of the initial distribution (A1). Some dependence on $P_{\rm nucl}^{(\alpha)}$ survives only in a restricted class of models where the landscape splits into a number of sectors with strictly zero probability of transitions between them and, in addition, where the maximum eigenvalue $\gamma_{\rm max}$ is degenerate. Even then, this dependence is limited to the relative probability of the sectors characterized by the eigenvalue $\gamma_{\rm max}$.

APPENDIX B: THE COLLAPSE DENSITY THRESHOLD δ_c

The collapse density threshold δ_c is determined by comparing the linearized evolution of matter perturbations with the nonlinear evolution of a spherical top-hat density perturbation, which can be treated as a closed FRW universe. The collapse density threshold $\delta_c(\tau)$ is defined as the amplitude reached by the linear evolution of an overdensity $\delta \equiv \delta\rho_m/\rho_m$ that has the same initial amplitude as a top-hat density perturbation that collapses to a singularity in proper time τ. In a matter-dominated universe with zero cosmological constant, δ_c is a constant; however, it is well known that δ_c depends on the collapse time when Λ is nonzero (see e.g. Refs. [54,55]). In this appendix we first outline the calculation of the time evolution of δ_c, then display the results for positive and negative Λ, and finally

describe how we apply it in our analysis of the collapse fraction F of Eq. (24).

As suggested by the definition above, both linear and nonlinear analyses are involved at different stages of the calculation of the collapse density. Arbitrarily small perturbations obey linearized equations of motion, and their evolution defines the linear growth function $G_\Lambda(\tau)$:

$$\delta(\tau) \propto G_\Lambda(\tau), \tag{B1}$$

where $G_\Lambda(\tau)$ is normalized so that the behavior for small τ is given by $G_\Lambda(\tau) \sim (3H_\Lambda\tau/2)^{2/3}$, where $H_\Lambda = \sqrt{|\Lambda|/3}$. The exact nonlinear analysis is used to determine the time at which an overdensity with a given initial amplitude will collapse to a singularity. For simplicity, this is worked out for the "top-hat" model, where the overdensity is assumed to be uniform and spherically symmetric. Such a region is embedded in a flat FRW universe containing only nonrelativistic matter and cosmological constant.

By Birkhoff's theorem, the evolution of the spherical overdensity is equivalent to that of a closed FRW universe. The Friedmann equation for a closed FRW universe, with scale factor a, may be written as

$$H^2 = H_\Lambda^2\left[\mathrm{sign}(\Lambda) + \frac{B(\kappa)}{a^3} - \frac{\kappa}{a^2}\right], \tag{B2}$$

where $H = d\ln a/d\tau = \dot{a}/a$ and $B(\kappa)$ is an arbitrary quantity that fixes the normalization of a. We will always choose $B(0) = 1$, so for $\kappa = 0$ the scale factor is normalized in such a way that $\rho_m = |\rho_\Lambda|$ at $a = 1$, where $\rho_\Lambda = \Lambda/(8\pi)$ is the vacuum energy density.

Let us first focus our attention on the evolution of a linearized density perturbation in a flat FRW universe with positive cosmological constant; the case with negative cosmological constant proceeds similarly. Consider a closed FRW universe obtained by "perturbing" the flat universe with a small curvature term $\delta\kappa$. The proper-time parameter $\hat{\tau}$ in such a universe, as a function of the scale factor, is given by an expansion with respect to the flat background: $\hat{\tau}(a) = \tau(a) + \delta\tau(a)$, where to linear order in $\delta\kappa$

$$\delta\tau(a) = \frac{\delta\kappa}{2H_\Lambda}\int_0^a \frac{\sqrt{a'}[a' - \frac{dB}{d\kappa}(0)]da'}{(1 + a'^3)^{3/2}}. \tag{B3}$$

The scale factor of the closed universe is obtained by inverting the function $\hat{\tau}(a)$:

$$\hat{a}(\tau) = a(\tau) - \dot{a}(\tau)\delta\tau(a(\tau)). \tag{B4}$$

As mentioned above, the evolution of this closed FRW universe also gives the evolution of a small density perturbation. Using $\rho_m = (3/8\pi)H_\Lambda^2 B(\kappa)/a^3$, one has

$$\delta = \frac{\delta\rho_m}{\rho_m} = -3\frac{\delta a}{a} + \frac{dB}{d\kappa}(0) = 3H\delta\tau + \frac{dB}{d\kappa}(0), \tag{B5}$$

where the last equality follows from Eq. (B4). From here on, unless noted otherwise, we normalize a so that $B(\kappa) = 1$. It is convenient to introduce the "time" variable

$$x \equiv \frac{|\rho_\Lambda|}{\rho_m} = a^3, \tag{B6}$$

for both choices of the sign of Λ. To be consistent with Eq. (B2), the solutions for $\kappa = 0$ are not normalized as in Eq. (21), but instead are given by

$$a(\tau) = \begin{cases} \sinh^{2/3}(\frac{3}{2}H_\Lambda\tau) & \text{for } \Lambda > 0 \\ \sin^{2/3}(\frac{3}{2}H_\Lambda\tau) & \text{for } \Lambda < 0. \end{cases} \tag{B7}$$

We can then find the evolution function $\delta(x)$ from Eq. (B5), using Eq. (B3) and also Eq. (B2) with $\kappa = 0$:

$$\delta(x) = \frac{1}{2}\delta\kappa\sqrt{1 + \frac{1}{x}}\int_0^x \frac{dy}{y^{1/6}(1 + y)^{3/2}} = \frac{3}{5}\delta\kappa G^+(x), \tag{B8}$$

where the linear growth function (for $\Lambda > 0$),

$$G^+(x) = \frac{5}{6}\sqrt{1 + \frac{1}{x}}\int_0^x \frac{dy}{y^{1/6}(1 + y)^{3/2}}, \tag{B9}$$

is normalized so that the behavior for small x is given by $G^+(x) \sim x^{1/3} = a \sim (3H_\Lambda\tau/2)^{2/3}$.

In the $\Lambda < 0$ case, the calculation proceeds along the same steps as before and the formula (B8) is indeed valid also for negative Λ, after replacing the growth function with $G^-(x)$. This function now has two branches $G_{\mathrm{I}}^-(x)$ and $G_{\mathrm{II}}^-(x)$, corresponding to the expanding and contracting phases of the universe, respectively. The first branch of the growth function introduces no new complications, and is found to be

$$G_{\mathrm{I}}^-(x) = \frac{5}{6}\sqrt{\frac{1}{x} - 1}\int_0^x \frac{dy}{y^{1/6}(1 - y)^{3/2}}. \tag{B10}$$

For the second branch, the integration is first performed over the whole history of the universe, from $x = 0$ to $x = 1$ and back to $x = 0$, and then one integrates back to the value of interest x. There is a complication, however, because for this case the denominator in Eq. (B3) is $(1 - a'^3)^{3/2}$, so the integral diverges when the upper limit is equal to 1. The cause of the problem is that for $\delta\kappa \neq 0$, $a_{\max}$ is no longer equal to 1. A simple cure is to choose $B(\kappa) = 1 + \kappa$ for this case, which ensures that $a_{\max} = 1$ for any κ, and which correspondingly provides an additional term in Eq. (B3) which causes the integral to converge. After some manipulation of the integrals, the result can be written as

$$G_{\mathrm{II}}^-(x) = \frac{5}{6}\sqrt{\frac{1}{x} - 1}\left[\frac{4\sqrt{\pi}\Gamma(\frac{5}{6})}{\Gamma(\frac{1}{3})} + \int_0^x \frac{dy}{y^{1/6}(1 - y)^{3/2}}\right]. \tag{B11}$$

The time dependence of the linear growth functions can be

made explicit by expressing x as a function of τ, through Eqs. (B6) and (B7).

In practice, we carry out our calculations using fitting functions for the growth functions, which were devised by Peacock [34], and which are accurate to better than 0.1%. These give

$$G_\Lambda^+(\tau) \simeq \tanh^{2/3}(\tfrac{3}{2}H_\Lambda\tau)[1-\tanh^{1.27}(\tfrac{3}{2}H_\Lambda\tau)]^{0.82} + 1.437H_\Lambda^{-2/3}[1-\cosh^{-4/3}(\tfrac{3}{2}H_\Lambda\tau)], \quad \text{(B12)}$$

$$G_\Lambda^-(\tau) \simeq (\tfrac{3}{2}H_\Lambda\tau)^{2/3}[1+0.37(\tau/\tau_{\rm crunch})^{2.18}]^{-1} \times [1-(\tau/\tau_{\rm crunch})^2]^{-1}, \quad \text{(B13)}$$

for the cases $\Lambda > 0$ and $\Lambda < 0$, respectively, where the latter fitting formula is valid for both branches.

We are now prepared to set the calculation of δ_c. Since the universe in Eq. (B2) can be viewed as a "perturbation" over a flat universe with $\delta\kappa = \kappa$, the time evolution of the overdensity is described in general by

$$\delta(\tau) = \tfrac{3}{5}\kappa G_\Lambda(\tau). \quad \text{(B14)}$$

The quantity $(3/5)\kappa a$ quantifies the size of the initial inhomogeneity.

In order to find the time at which the spherical overdensity collapses, it is convenient to determine the time of turnaround $\tau_{\rm turn}$, corresponding to when $H = 0$. The time of collapse is then given by $2\tau_{\rm turn}$. The turnaround time is obtained by integrating Eq. (B2), choosing $B = 1$:

$$H_\Lambda\tau_{\rm turn}(\kappa) = \int_0^{a_{\rm turn}(\kappa)} \frac{\sqrt{a}da}{\sqrt{{\rm sign}(\Lambda)a^3 - \kappa a + 1}}, \quad \text{(B15)}$$

where the scale factor at turnaround $a_{\rm turn}$ corresponds to the smallest positive solution of

$${\rm sign}\,(\Lambda)a_{\rm turn}^3 - \kappa a_{\rm turn} + 1 = 0. \quad \text{(B16)}$$

For positive Λ, the universe will collapse only if $\kappa > \kappa_{\rm min} \equiv 3/2^{2/3}$; for negative Λ, perturbations that collapse before the universe has crunched have $\kappa > 0$.

The numerical evaluation of the integral in Eq. (B15) allows one to extract the function $\tau_{\rm turn}(\kappa)$, which can be inverted to give $\kappa_{\rm turn}(\tau)$, expressing the value of κ that leads to turnaround at time τ. Finally, the collapse density threshold as a function of the time of collapse is read from Eq. (B14):

$$\delta_c(\tau) = \tfrac{3}{5}\kappa_{\rm turn}(\tau/2)G_\Lambda(\tau). \quad \text{(B17)}$$

In the limits of small and large collapse times the above procedure can be carried out analytically to find the limiting values of δ_c. Let us consider first the large-time regime, corresponding to small κ. In the case $\Lambda > 0$, the smallest κ allowed is $\kappa_{\rm min}$; therefore

$$\delta_c^+(\infty) = \tfrac{3}{5}\kappa_{\rm min}G_\Lambda^+(\infty) \simeq 1.629, \quad \text{(B18)}$$

where $G_\Lambda^+(\infty) = G^+(\infty) = 5\Gamma(2/3)\Gamma(5/6)/(3\sqrt{\pi}) \simeq 1.437$. The case $\Lambda < 0$ is a little more complicated. The collapse time cannot exceed $\tau_{\rm crunch} = 2\pi/3H_\Lambda$, corresponding to $\kappa = 0$. At small κ, the integral in Eq. (B15) is expanded to give

$$H_\Lambda\tau_{\rm turn}(\kappa) \simeq \frac{1}{2}H_\Lambda\tau_{\rm crunch} - \frac{2}{5}\frac{\sqrt{\pi}\Gamma(\frac{11}{6})}{\Gamma(\frac{1}{3})}\kappa. \quad \text{(B19)}$$

On the other hand, the growth function $G^-(\tau)$ in the neighborhood of $\tau_{\rm crunch}$ behaves as

$$G_\Lambda^-(\tau \approx \tau_{\rm crunch}) \simeq \frac{10}{3}\frac{\Gamma(\frac{5}{6})}{\sqrt{\pi}\Gamma(\frac{1}{3})}\frac{1}{(1-\tau/\tau_{\rm crunch})}. \quad \text{(B20)}$$

After using Eqs. (B19) and (B20) in the general formula (B17), we simply get

$$\delta_c^-(\tau_{\rm crunch}) = 2. \quad \text{(B21)}$$

In the opposite regime $H_\Lambda\tau \ll 1$, corresponding to large κ, the growth functions are $G_\Lambda^\pm(\tau) \simeq a(\tau) \simeq (3H_\Lambda\tau/2)^{2/3}$. The integral (B15) can be analytically solved in this limit: $H_\Lambda\tau_{\rm turn}(\kappa) = \pi/(2\kappa^{3/2})$. Combining these results leads to

$$\delta_c^\pm(0) = \frac{3}{5}\left(\frac{3\pi}{2}\right)^{2/3} \simeq 1.686, \quad \text{(B22)}$$

which is also the constant value of δ_c in a $\Lambda = 0$ universe.

The time dependence of δ_c is displayed in Fig. 6, for both positive and negative values of Λ. We also display the following simple fitting functions:

$$\delta_c^+(\tau) = 1.629 + 0.057e^{-0.28H_\Lambda^2\tau^2},$$
$$\delta_c^-(\tau) = 1.686 + 0.165\left(\frac{\tau}{\tau_{\rm crunch}}\right)^{2.5} + 0.149\left(\frac{\tau}{\tau_{\rm crunch}}\right)^{11} \quad \text{(B23)}$$

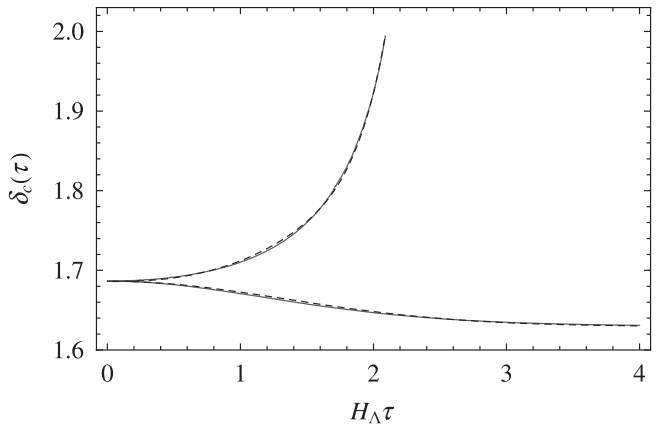

FIG. 6. The collapse density thresholds δ_c^+ (for $\Lambda > 0$) and δ_c^- (for $\Lambda < 0$), as functions of time. The solid curves represent numerical evaluations of $\delta_c^\pm$, while the dashed curves correspond to the fitting functions in Eq. (B23). Note that δ_c^+ decreases with time, while δ_c^- increases with time.

which are accurate to better than 0.2%. Although we choose to include the effect of the time evolution of δ_c, our results are not significantly changed by treating δ_c as a constant. This is easy to understand. First of all, δ_c^+ varies by only about 3%. The evolution of δ_c^- is more significant, about 15%, and most of this happens at very late times. But our anthropic weight in Eq. (20) never samples δ_c^- within a time $\Delta\tau$ of $\tau_{\rm crunch}$.

Finally, we point out that the appearance of $G_\Lambda(\tau)$ in this discussion is not needed for the calculation, and appears here primarily to make contact with other work. From Eq. (24) one sees that the collapse fraction depends only on the ratio of $\delta_c(\tau)/\sigma(M_G, \tau)$, which from Eqs. (25) and (B17) can be seen to equal $(3/5)\kappa_{\rm turn}(\tau/2)/\bar{\sigma}(M_G)$. Expressed in this way, Eq. (24) becomes fairly transparent. Since κ is a measure of the amplitude of an initial perturbation, Eq. (24) is saying that the collapse fraction at time τ depends precisely on the magnitude required for an initial top-hat perturbation to collapse by time τ. In more detail, Eq. (24) is predicated on a Gaussian distribution of initial fluctuations, where the complementary error function erfc(x) is the integral of a Gaussian. The collapsed fraction at time τ is given by the probability, in this Gaussian approximation, for the initial fluctuations to exceed the magnitude needed for collapse at time τ. From a practical point of view, the use of $G_\Lambda(\tau)$ in the discussion of the collapse fraction can be a helpful simplification if one uses the approximation that $\delta_c \approx$ const. We have not used this approximation, but as described above, our results would not be much different if we had. We have maintained the discussion in terms of $G_\Lambda(\tau)$ to clarify the relationship between our work and this approximation.

[1] S. Winitzki, Lect. Notes Phys. **738**, 157 (2008).
[2] A. H. Guth, Phys. Rep. **333**, 555 (2000).J. Phys. A **40**, 6811 (2007).
[3] A. Linde, Lect. Notes Phys. **738**, 1 (2008).
[4] A. Vilenkin, J. Phys. A **40**, 6777 (2007).
[5] A. Aguirre, S. Gratton, and M. C. Johnson, Phys. Rev. Lett. **98**, 131301 (2007).
[6] J. Garcia-Bellido, A. D. Linde, and D. A. Linde, Phys. Rev. D **50**, 730 (1994); J. Garcia-Bellido and A. D. Linde, Phys. Rev. D **51**, 429 (1995); **52**, 6730 (1995).
[7] A. Vilenkin, Phys. Rev. Lett. **74**, 846 (1995).
[8] A. Linde, J. Cosmol. Astropart. Phys. 01 (2007) 022.
[9] A. D. Linde and A. Mezhlumian, Phys. Lett. B **307**, 25 (1993).
[10] A. D. Linde, D. A. Linde, and A. Mezhlumian, Phys. Rev. D **49**, 1783 (1994).
[11] A. Vilenkin, Phys. Rev. D **52**, 3365 (1995).
[12] A. Linde, J. Cosmol. Astropart. Phys. 06 (2007) 017.
[13] J. Garriga, T. Tanaka, and A. Vilenkin, Phys. Rev. D **60**, 023501 (1999).
[14] A. Vilenkin, Phys. Rev. Lett. **81**, 5501 (1998); V. Vanchurin, A. Vilenkin, and S. Winitzki, Phys. Rev. D **61**, 083507 (2000).
[15] J. Garriga, D. Schwartz-Perlov, A. Vilenkin, and S. Winitzki, J. Cosmol. Astropart. Phys. 01 (2006) 017.
[16] R. Easther, E. A. Lim, and M. R. Martin, J. Cosmol. Astropart. Phys. 03 (2006) 016.
[17] R. Bousso, Phys. Rev. Lett. **97**, 191302 (2006); R. Bousso, B. Freivogel, and I. S. Yang, Phys. Rev. D **74**, 103516 (2006).
[18] L. Susskind, arXiv:0710.1129.
[19] V. Vanchurin, Phys. Rev. D **75**, 023524 (2007).
[20] S. Winitzki, arXiv:gr-qc/0803.1300 [Phys. Rev. D (to be published)].
[21] A. D. Linde, D. A. Linde, and A. Mezhlumian, Phys. Lett. B **345**, 203 (1995).
[22] R. Bousso, B. Freivogel, and I. S. Yang, Phys. Rev. D **77**, 103514 (2008).
[23] B. Feldstein, L. J. Hall, and T. Watari, Phys. Rev. D **72**, 123506 (2005).
[24] J. Garriga and A. Vilenkin, Prog. Theor. Phys. Suppl. **163**, 245 (2006).
[25] M. L. Graesser and M. P. Salem, Phys. Rev. D **76**, 043506 (2007).
[26] S. Weinberg, Phys. Rev. Lett. **59**, 2607 (1987).
[27] A. D. Linde, Rep. Prog. Phys. **47**, 925 (1984).
[28] A. D. Linde, in *Three Hundred Years of Gravitation*, edited by S. W. Hawking and W. Israel (Cambridge University Press Cambridge, England, 1987).
[29] G. Efstathiou, Mon. Not. R. Astron. Soc. **274**, L73 (1995).
[30] H. Martel, P. R. Shapiro, and S. Weinberg, Astrophys. J. **492**, 29 (1998).
[31] J. Garriga, M. Livio, and A. Vilenkin, Phys. Rev. D **61**, 023503 (1999).
[32] M. Tegmark, A. Aguirre, M. J. Rees, and F. Wilczek, Phys. Rev. D **73**, 023505 (2006).
[33] L. Pogosian and A. Vilenkin, J. Cosmol. Astropart. Phys. 01 (2007) 025.
[34] J. A. Peacock, Mon. Not. R. Astron. Soc. **379**, 1067 (2007).
[35] R. Bousso, R. Harnik, G. D. Kribs, and G. Perez, Phys. Rev. D **76**, 043513 (2007).
[36] J. M. Cline, A. R. Frey, and G. Holder, Phys. Rev. D **77**, 063520 (2008).
[37] A. A. Starobinsky, in: *Current Topics in Field Theory, Quantum Gravity and Strings*, edited by H. J. de Vega and N. Sanchez, Lecture Notes in Physics Vol. 206 (Springer, New York, 1986), p. 107.
[38] A. Vilenkin, Phys. Rev. D **27**, 2848 (1983).
[39] A. D. Linde, Phys. Lett. B **175**, 395 (1986).
[40] J. R. Gott, Nature (London) **295**, 304 (1982).
[41] P. J. Steinhardt, in *The Very Early Universe*, edited by G. W. Gibbons, S. W. Hawking, and S. T. C. Siklos (Cambridge University Press, Cambridge, England, 1983).

[42] J. Garriga and A. Vilenkin, Phys. Rev. D **57**, 2230 (1998).
[43] S. R. Coleman and F. De Luccia, Phys. Rev. D **21**, 3305 (1980).
[44] A. Vilenkin and S. Winitzki, Phys. Rev. D **55**, 548 (1997).
[45] D. Schwartz-Perlov and A. Vilenkin, J. Cosmol. Astropart. Phys. 06 (2006) 010; D. Schwartz-Perlov, J. Phys. A **40**, 7363 (2007).
[46] M. Tegmark and M. J. Rees, Astrophys. J. **499**, 526 (1998).
[47] L. J. Hall, T. Watari, and T. T. Yanagida, Phys. Rev. D **73**, 103502 (2006).
[48] A. Linde and V. Mukhanov, J. Cosmol. Astropart. Phys. 04 (2006) 009.
[49] B. Freivogel, M. Kleban, M. Rodriguez Martinez, and L. Susskind, J. High Energy Phys. 03 (2006) 039.
[50] A. De Simone, A. H. Guth, M. P. Salem, and A. Vilenkin (unpublished).
[51] K. D. Olum and D. Schwartz-Perlov, J. Cosmol. Astropart. Phys. 10 (2007) 010.
[52] T. Clifton, S. Shenker, and N. Sivanandam, J. High Energy Phys. 09 (2007) 034.
[53] W. H. Press and P. Schechter, Astrophys. J. **187**, 425 (1974); J. M. Bardeen, J. R. Bond, N. Kaiser, and A. S. Szalay, Astrophys. J. **304**, 15 (1986).
[54] P. B. Lilje, Astrophys. J. **386**, L33 (1992); S. D. M. White, G. Efstathiou, and C. S. Frenk, Mon. Not. R. Astron. Soc. **262**, 1023 (1993).V. R. Eke, S. Cole, and C. S. Frenk, Mon. Not. R. Astron. Soc. **282**, 263 (1996).
[55] M. Tegmark, A. Vilenkin, and L. Pogosian, Phys. Rev. D **71**, 103523 (2005).
[56] A. Jenkins *et al.*, Mon. Not. R. Astron. Soc. **321**, 372 (2001).
[57] R. K. Sheth and G. Tormen, Mon. Not. R. Astron. Soc. **308**, 119 (1999); R. K. Sheth, H. J. Mo, and G. Tormen, Mon. Not. R. Astron. Soc. **323**, 1 (2001).
[58] M. S. Warren, K. Abazajian, D. E. Holz, and L. Teodoro, Astrophys. J. **646**, 881 (2006).
[59] G. Kauffmann *et al.* (SDSS Collaboration), Mon. Not. R. Astron. Soc. **341**, 54 (2003).
[60] J. Dunkley *et al.* (WMAP Collaboration), arXiv:0803.0586; E. Komatsu *et al.* (WMAP Collaboration), arXiv:0803.0547.
[61] U. Seljak and M. Zaldarriaga, Astrophys. J. **469**, 437 (1996).
[62] A. Loeb, J. Cosmol. Astropart. Phys. 05 (2006) 009.
[63] S. A. Bludman, Nucl. Phys. **A663**, 865 (2000).
[64] A. Albrecht and L. Sorbo, Phys. Rev. D **70**, 063528 (2004); D. N. Page, J. Korean Phys. Soc. **49**, 711 (2006); D. N. Page, arXiv:hep-th/0610079; R. Bousso and B. Freivogel, J. High Energy Phys. 06 (2007) 018.
[65] A. De Simone, A. H. Guth, A. Linde, M. Noorbala, M. P. Salem, and A. Vilenkin (work in progress).
[66] A. Vilenkin, Phys. Rev. D **30**, 509 (1984); **33**, 3560 (1986); A. D. Linde, Lett. Nuovo Cimento Soc. Ital. Fis. **39**, 401 (1984); V. A. Rubakov, Phys. Lett. B **148**, 280 (1984).
[67] J. B. Hartle and S. W. Hawking, Phys. Rev. D **28**, 2960 (1983).